Catalysis Letters Vol. 110, Nos. 1–2, August 2006 (© 2006)
DOI: 10.1007/s10562-006-0103-1

Liquid-phase oxidation of toluene by molecular oxygen over copper manganese oxides

Xiaoqiang Li, Jie Xu,* Lipeng Zhou, Feng Wang, Jin Gao, Chen Chen, Jianbo Ning, and Hong Ma

State Key Laboratory of Catalysis, Dalian Institute of Chemical Physics, Graduate School of the Chinese Academy of Sciences, Chinese Academy of Sciences, 457 Zhongshan Road, P.O.Box 110, Dalian 116023, P.R. China

Received 19 March 2006; accepted 24 May 2006

Copper manganese oxides (Cu–Mn oxides) were prepared by coprecipitation method and characterized by several techniques, such as X-ray powder diffraction (XRD), Fourier transform infrared spectroscopy (FT-IR) and Temperature-programmed reduction (TPR). Catalytic activities of the Cu–Mn oxides were tested by the oxidation of toluene with molecular oxygen in liquid phase and solvent-free conditions. The molar ratio of Cu:Mn in catalyst was optimized to be 1:1 and thus the corresponding crystalline material was designated as $Cu_{1.5}Mn_{1.5}O_4$.

KEY WORDS: toluene; oxidation; Cu–Mn Oxide; solvent-free; $Cu_{1.5}Mn_{1.5}O_4$.

1. Introduction

Catalytic oxidation is an important technology for the conversion of hydrocarbon feedstocks to industrially important oxygenated derivatives. [1] For example, selective catalytic oxidation of methylbenzenes to corresponding alcohols, aldehydes and carboxylic acid by molecular oxygen is of great economic and industrial importance [1,2]. For instance, industrial grade benzoic acid is used as a chemical intermediate and as a diverting agent in crude-oil recovery applications, in addition, the oxidation of toluene to benzoic acid with O_2 is a key step for synthesizing ε-caprolactamin in Snia-Viscosa process[3,4]. Presently, the principal industrial production of benzoic acid via oxidation of toluene employ homogeneous cobalt catalysts in an air pressurized aqueous acetic acid mixture in the presence of Mn ions and bromide promoters [5]. The use of acetic acid solvent and promoters may bring difficulties for the separation of catalysts and products, equipment corrosion and large volume of acidic waste. Many reports involved the oxidation of toluene by vapor-phase oxidation using vanadium or molybdenum as catalysts[6–9]. However, liquid-phase oxidation is easy to operate and to achieve high selectivity under the relatively mild reaction conditions. Many efforts have been made to improve the efficiency of toluene oxidation in liquid phase through the addition of Mn ions or the use of supercritical CO_2 solvent[10–13]. NHPI/$Co(Ac)_2{\cdot}4H_2O$ was reported as a catalytic system of oxidation of toluene in acetic acid[14,15]. However, most investigations still focus on homogeneous systems, and volatile solvents employed are all the same. In contrast, by employing heterogeneous catalysts in liquid-phase oxidation of toluene, especially without a solvent, those drawbacks could be overcome, and the process would be more environmentally friendly.

Copper manganese mixed oxides have been investigated as efficient catalysts for the oxidation of carbon monoxide[16–21]. The success of the copper manganese mixed oxide catalysts have prompted a great deal of fundamental work devoted to clarifying the role played by each component and the nature of the active sites. Copper manganese oxides have generally been observed to lose activity for CO oxidation at temperature above 500 °C when crystallization of the spinel occurs[22]. However, crystalline $Cu_{1+x}Mn_{2-\rm x}O_4$ has also been shown to be an active catalyst for CO oxidation at suitable temperatures[23]. In addition, copper manganese oxides were also catalysts for the oxidation of ammonia and other gas species[24]. Recently, copper manganese oxides supported on activated carbon were reported as efficient catalysts for the oxidation of p-cresol[25,26].

In this work, we found that Cu–Mn oxides catalysts could catalyze the liquid-phase oxidation of toluene using molecular oxygen without the use of a solvent and an additive. The use of a heterogeneous catalyst in the solvent-free condition has the advantages of minimizing separation difficulty and equipment corrosion. Investigation of the effects such as metal ratio, calcination temperature and reaction time provides the insights for the oxidation reaction over the catalysts.

*To whom correspondence should be addressed.
E-mail: xujie@dicp.ac.cn

2. Experimental

2.1. Preparation of copper manganese oxides

Copper manganese oxides catalysts and other Cu- and Mn-based catalysts were prepared by the co-precipitation method. Typically, Cu–Mn oxide with the 1:1 ratio was prepared by the following procedure: 0.1 mol copper acetate (19.9 g) and 0.1 mol manganese acetate (24.5 g) were dissolved into deionized water, and then the solution of 0.2 mol sodium carbonate (20.1 g) was dropped under stirring. The mixture was vigorously stirred for 4 h at room temperature. The solid was obtained by filtration and then washed with deionized water for several times. After drying at 120 °C for 10 h, the solid was calcined at 500 °C for 6 h.

The molar ratio of Cu to Mn is varied from 5:1 to 1:2. As calcination of the catalysts leads to the formation of crystalline phase, we examined the effect of calcination temperature (400–800 °C) for the samples with the Cu:Mn molar ratio at 1:1. The catalysts are labeled CuAMnB-X, where the molar ratio Cu:Mn = A:B and X denoted the catalyst calcined at X °C.

2.2. Characterization of the catalysts

The crystalline phase of the catalysts were determined by X-ray powder diffraction (XRD) using a Rigaku Miniflex diffractometer employing Cu-Kα radiation. Crystallinity of the Cu–Mn oxides is defined as $C_i = 100\ S_i/S_{max}$, where i represents the calcination temperature of the Cu–Mn oxides. S_i is the summation of the integral areas of prominent peaks of the spinel $Cu_{1+x}Mn_{2-x}O_4$. S_{max} is the maximum S_i in S_{500}, S_{600}, S_{700}, and S_{800}. Temperature-programmed reduction (TPR) was carried out by feeding 5% H_2 in N_2 to 35 mg of catalyst in a conventional flow reactor without prior oxidation treatment. The flow rate of the reducing gas was set at 54 mL/min. The temperature of reaction was raised from room temperature to 820 °C at a rate of 20 °C/min. The rate of H_2 consumption was determined by using a thermal conductivity detector and recorded on an on-line personal computer. The FT-IR spectra were measured on a Bruker Tensor 27 FT-IR spectrometer after 32 scans for a resolution of 4 cm^{-1} in KBr media.

2.3. Evaluation of catalytic activity

The oxidation reaction was carried out in a stirred 500 mL autoclave. In a typical reaction, toluene (50 mL, 0.6 mol) and catalyst (1.0 g) were placed in the reactor and mixed by the impeller. After sealed, the reactor was heated up to a set temperature by an electric furnace. After the desired temperature was reached, oxygen was charged to the reactor through a dip tube. The pressure was kept constant by supplying oxygen gas during the reaction. After a certain term of reaction, the reaction mixture was cooled and dissolved in 50 mL ethanol, and then catalyst was separated by filtration. The reaction products were analyzed by an Agilent model 4890D gas chromatograph. A PEG-20M capillary column (50 m × 0.32 mm × 0.4 μm) was used for the separation of products. Quantification of components was performed by using 1,2,4,5-tetramethylbenzene as an internal standard. The conversion and product distribution were evaluated with calibration curves.

3. Results and discussion

3.1. Characterization of the catalysts

3.1.1. X-ray powder diffraction (XRD)

Figure 1 shows the XRD patterns of CuAMnB-500. The main crystalline phase of the Cu1Mn1-500 was $Cu_{1.5}Mn_{1.5}O_4$ (with a very little amount of CuO, indicating that the $Cu_{1.5}Mn_{1.5}O_4$ was not stoichiometric). Cu2Mn1-500 was composed of non-stoichiometric $Cu_{1.5}Mn_{1.5}O_4$ phase and CuO phase. The catalyst Cu5Mn1-500 was also composed of $Cu_{1.5}Mn_{1.5}O_4$ and CuO phases. For Cu1Mn2-500, a minor Mn_2O_3 phase was detected together with a predominant $Cu_{1.5}Mn_{1.5}O_4$ phase. The conclusion was that $Cu_{1.5}Mn_{1.5}O_4$ phase exists in all the catalyst crystalline. The addition of copper resulted in the formation of CuO phase and the addition of manganese resulted in the formation of Mn_2O_3 phase.

The crystallite structure of the Cu1Mn1-X (Cu:Mn molar ratio was 1:1) catalysts were revealed by XRD analysis as shown in figure 2. Results clearly showed that all the crystalline phases of the Cu1Mn1-X (X > 500) catalysts consist of that $Cu_{1.5}Mn_{1.5}O_4$ phase (also with a very little amount of CuO, like Cu1Mn1-500), and only Cu1Mn1-800 has a minor Mn_2O_3 phase. It is strange that the peaks of CuO phase was not clearly recognized in the XRD patterns of Cu1Mn1-800 sample,

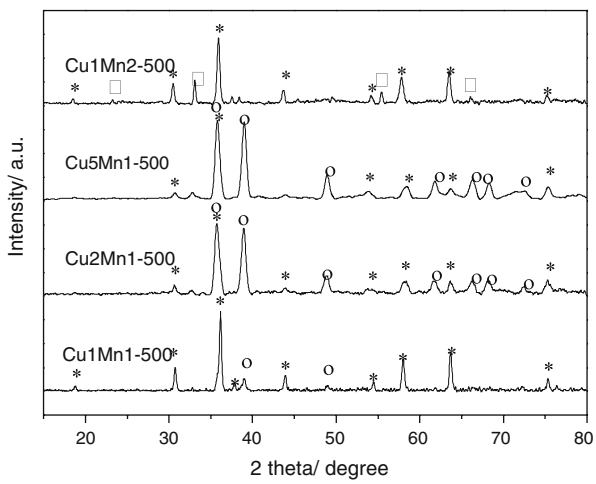

Figure 1. XRD patterns of CuAMnB-500. (*) $Cu_{1.5}Mn_{1.5}O_4$, (○) CuO (□) Mn_2O_3.

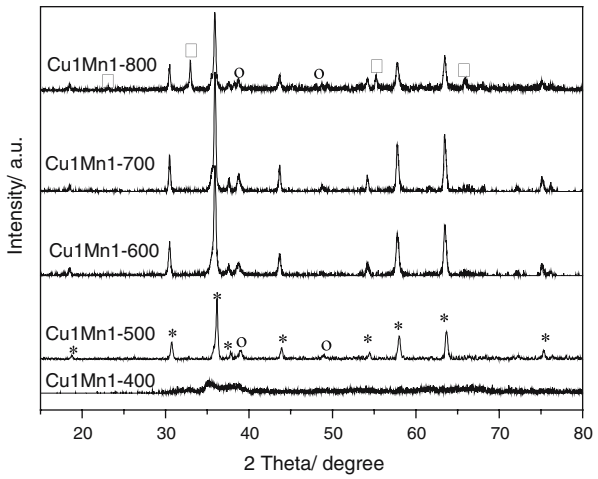

Figure 2. XRD patterns of Cu1Mn1-X catalysts. (□)Mn_2O_3 (*) $Cu_{1.5}Mn_{1.5}O_4$ (o) CuO.

although the original Cu:Mn ratio was 1:1. Zheng and his co-workers [27] reported that Cu–Mn oxides would form high-dispersed CuO at high temperatures which could help to explain the phenomenon: CuO was formed after calcinations at 800 °C but its diffraction peaks were broadened due to high dispersion.

The main crystalline phase, the percent of crystallinity and the crystallite size of $Cu_{1.5}Mn_{1.5}O_4$ in CuAMnB-X were listed in Table 1. Among the CuAMnB-500 samples (calcined at 500 °C with different Cu:Mn ratios), the Cu1Mn1-500 has better crystallinity of $Cu_{1.5}Mn_{1.5}O_4$phase than other samples. The superabundance of copper and manganese both decreased the crystallinity and other phases such as CuO and Mn_2O_3 might form. The crystallinity of Cu1Mn1-600 is higher than others in the Cu1Mn1-X series of samples. The $Cu_{1.5}Mn_{1.5}O_4$ could not be formed when the sample was calcined at 400 °C. The crystallinity of Cu1Mn1-700 was similar to that of Cu1Mn1-600. However, the crystallinity of Cu1Mn1-800 was lower than that of Cu1Mn1-600 due to the structure changes at the high temperature.

3.1.2. Fourier transform infrared (FT-IR)

The FT-IR spectra of Cu1Mn1-X were shown in figure 3. Compared with the results of D. Mehandjiev [28] and co-workers, who investigated the FT-IR spectra of copper manganese oxides, the peak at 530 cm^{-1} was assigned the absorption of Mn–O in the spinel structure. The peaks at 504 and 478 cm^{-1} were attributed to the absorption of the Cu–O in the spinel structure. The spectrum of Cu1Mn1-500 was very close to that shown in reference [28,29] for octahedral $Cu_{1.5}Mn_{1.5}O_4$ phase. The spectra of Cu1Mn1-600 and Cu1Mn1-700 samples were similar to that of Cu1Mn1-500. Cu1Mn1-400 has different spectrum because of its amorphous structure and the peak at 860 cm^{-1} was assigned to the distortion vibration of CO_3^{2-}. The spectrum of Cu1Mn1-800 showed the absorption bands of $Cu_{1.5}Mn_{1.5}O_4$ phase and others at about 620 cm^{-1}, which attributed to the Mn–O stretch vibration in the Mn_2O_3 phase.

3.1.3. Temperature-programmed reduction (TPR)

Figure 4 comprises TPR profiles of Cu1Mn1-X samples. The Cu1Mn1-400 exhibited three peaks at 170C, 275 and 320 °C, which can be ascribed to the reduction of CuO and the two reduction stages from Mn_2O_3 to MnO via Mn_3O_4[30,31]. The XRD and FT-IR results showed above indicated that Cu1Mn1-400 did not form the $Cu_{1.5}Mn_{1.4}O_4$ phase; and the TPR profile also showed that both CuO and Mn_2O_3 existed in the sample. The reduction of Cu1Mn1-600 exhibited a broad peak around 460 °C, comprising the reduction of manganese and copper oxides, though it is hard to define a clear boundary between the regions. It is likely that the higher calcination temperature resulted in the better crystallinity as the XRD analysis suggested and the copper and manganese cations were partly reduced at the same temperature region[32]. The reduction of Cu1Mn1-500 was similar to that of Cu1Mn1-600 except the shoulder peak at 210 °C, which was the signal from the reduction of CuO. The TPR profile of Cu1Mn1-700 showed two reduction peaks at 315 and 420 °C. According to Vandenberghe[33], it has been established that the redox process $Cu^{2+} + Mn^{3+} = Cu^{+} + Mn^{4+}$

Table 1
Properties of CuAMnB-X samples after calcination

Sample	Calcination temperature (°C)	Molar ratio Cu:Mn	Main crysalline phase	Crystallinity (%)	Crystallite size[a] (nm)
Cu5Mn1-500	500	5:1	$Cu_{1.5}Mn_{1.5}O_4$,CuO	–	–
Cu2Mn1-500	500	2:1	$Cu_{1.5}Mn_{1.5}O_4$,CuO	–	–
Cu1Mn1-500	500	1:1	$Cu_{1.5}Mn_{1.5}O_4$	83	33
Cu1Mn2-500	500	1:2	$Cu_{1.5}Mn_{1.5}O_4$,Mn_2O_3	65	28
Cu1Mn1-400	400	1:1	–	–	–
Cu1Mn1-600	600	1:1	$Cu_{1.5}Mn_{1.5}O_4$	100	34
Cu1Mn1-700	700	1:1	$Cu_{1.5}Mn_{1.5}O_4$	94	37
Cu1Mn1-800	800	1:1	$Cu_{1.5}Mn_{1.5}O_4$,Mn_2O_3	59	38

[a] Crystallite size was obtained for the 311 peak by the sherrere equation.

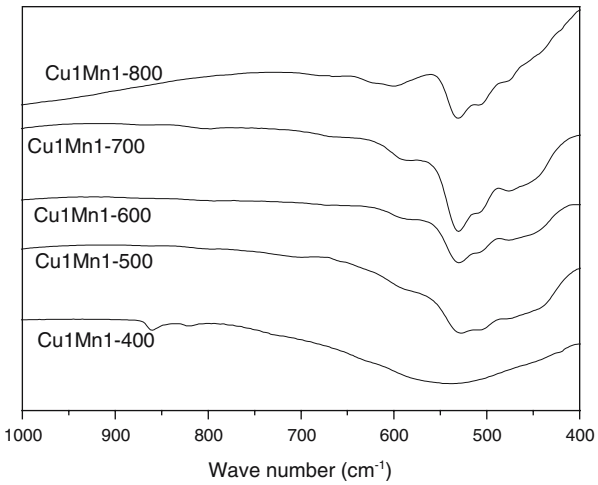

Figure 3. FT-IR spectra of Cu1Mn1-X.

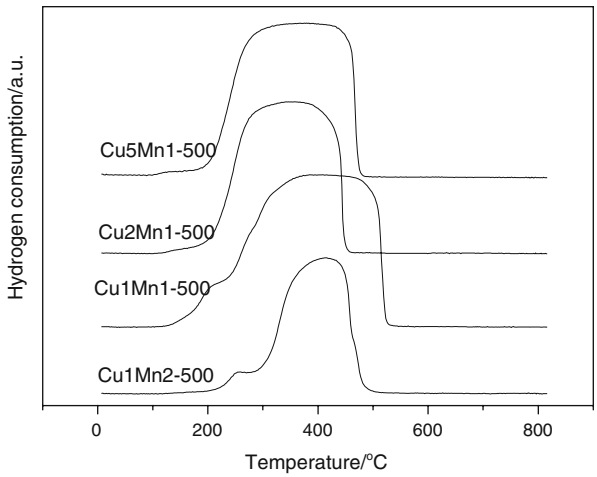

Figure 5. TPR profiles of CuAMnB-500.

play an important role with the spinel structure. At low temperatures, the equilibrium was shifted to the left, while at higher temperatures, a shift to the right was predominant, favoring the formation of Cu^{+} and Mn^{4+}. The shift of the equilibrium to the right caused the increase of the amount of Cu^{+} and Mn^{4+}, and complicated the reduction of Cu1Mn1-700 and Cu1Mn1-800. It is observed that the reduction peaks shift to higher temperatures upon calcination at higher temperatures.

Figure 5 comprises TPR profiles of Cu–Mn oxides with different Cu:Mn ratios. The TPR profile of Cu2Mn1-500 and Cu5Mn1-500 exhibited a broad peak due to the reduction of spinel copper manganese oxides. The temperature of the reduction starts to decrease when the Cu content increased, indicating that manganese oxide retarded the reduction of copper oxide. A similar effect was reported by Wöllner and co-workers when investigating the TPR of copper manganese oxide catalysts, and besides, the effect was also reported by Leith and co-workers on the iron manganese oxides[24,34]. The temperature to finish the reduction of Cu1Mn1-500 was higher than those of other samples. The high crystallinity of $Cu_{1.5}Mn_{1.5}O_4$ (Table 1) in the sample might cause the reduction of the copper manganese oxides more difficult.

3.2. Catalytic activities of the catalysts

3.2.1. Catalytic activities of Cu1Mn1-500 compared with other catalysts

The conversions of toluene oxidation over Cu1Mn1-500 catalyst and other Copper-based and manganese-based catalysts were shown in figure 6. The products of the reaction were benzaldehyde, benzyl alcohol and benzoic acid. By-products were benzyl benzoate and others in a low concentration. The catalytic results of all the mixed oxides in figure 6 displayed that the copper manganese oxides had higher catalytic activity than other bimetal oxide catalysts for the oxidation of toluene.

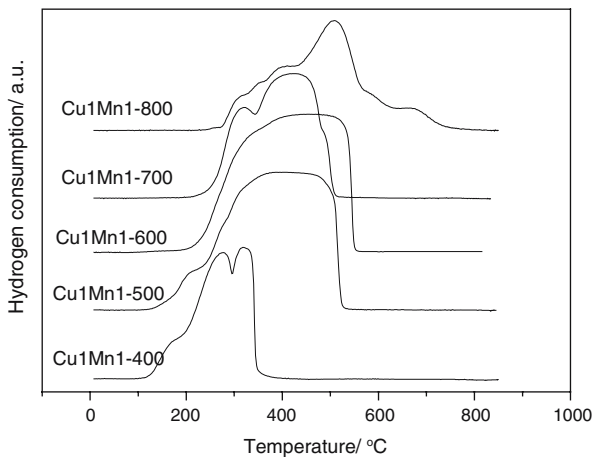

Figure 4. TPR profiles of Cu1Mn1-X.

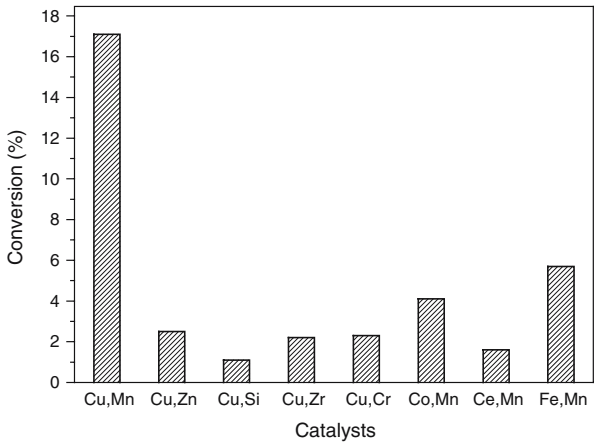

Figure 6. The conversions of toluene oxidation over bi-metallic oxides catalysts (Reaction conditions: 1.0 g catalysts, 50 mL toluene, 1.0 MPa O_2 , 2 h, 190 °C).

3.2.2. Catalytic activity of copper manganese oxides catalysts

Table 2 showed toluene aerobic oxidation activity over CuAMnB-X catalysts. About the CuAMnB-500 catalysts, the order of activity for the toluene oxidation was, Cu1Mn1-500 > Cu2Mn1-500 > Cu1Mn2-500 > Cu5Mn1-500. It is concluded that the optimum molar ratio of Cu:Mn was 1:1, and the superabundant of Cu or Mn would decrease the activity. According to the data in Table 1, we know that Cu1Mn1-500 mainly consisted of $Cu_{1.5}Mn_{1.5}O_4$, which may be the active phase for the oxidation reaction. The calcination process of the copper manganese oxides leads to the formation of crystalline phases, upon that we examined the activity of toluene oxidation over Cu1Mn1-X catalysts at the same condition. Cu1Mn1-400 was amorphous copper and manganese mixed oxides, which showed a low activity for the oxidation of toluene. Three catalysts (Cu1Mn1-500, Cu1Mn1-600 and Cu1Mn1-700) had the high crystallinity of $Cu_{1.5}Mn_{1.5}O_4$, and the conversions of the reaction were 17.2%, 17.6%, and 17.4%, respectively. From the result in Table 2 we know that the catalyst with the Cu:Mn ratio of 1:1 had the higher catalytic activity than the other copper manganese oxides with other Cu:Mn ratios; and the catalyst with high crystallinity of $Cu_{1.5}Mn_{1.5}O_4$ also had higher catalytic activity than the catalyst with amorphous or poor crystallinity. It is concluded that the spinel $Cu_{1.5}Mn_{1.5}O_4$ was the active phase of the copper manganese oxides in the liquid-phase toluene oxidation reaction.

3.3. The effect of reaction time

Figure 7 shows the time course of catalytic performance in the toluene oxidation over Cu1Mn1-700 catalyst. From figure 7 we could find that the conversion increases with the time and increased more rapidly from 60 min to 90 min than other periods. At the reaction time of 60 min, the main products are benzaldehyde, benzyl alcohol and benzoic acid at about 1:1:1 ratio. After the rapid reaction period between 60 and 90 min, the selectivity of benzaldehyde decreased with the time. The change of the selectivity of benzyl alcohol was similar to the benzaldehyde except for that the concentrate of alcohol was very low at last (180 min). After 30 min, the selectivity of benzoic acid increased with the reaction time and the increased slowly after 90 min, which was similar to the change of conversion. These results showed that benzoic acid was the deep oxidation product of benzyl alcohol and benzaldehyde. Benzyl benzoate appeared after 60 min, and increased with the time. The reaction rate became slow after 90 min but the benzyl benzoate increased rapidly, along with the decrease of selectivity to alcohol. It is concluded that benzyl benzoate was the esterification product of the benzoic acid and benzyl alcohol. After 90 min, some other products appeared but with low concentrations.

Table 2
the results of toluene oxidation over Cu–Mn oxides catalysts[a]

Entry	Catalyst	Conv. (mol %)	Product distribution (mol %)				
			BAL[b]	BOL	BAC	BB	Others
1	Cu5Mn1-500	4.8	28.7	28.9	34.2	5.2	3.0
2	Cu2Mn1-500	11.8	16.8	20.5	50.1	10.8	1.8
3	Cu1Mn1-500	17.2	11.7	18.7	63.1	3.1	3.5
4	Cu1Mn2-500	6.6	24.9	29.4	38.7	4.3	2.7
5	Cu1Mn1-400	3.2	64.1	18.3	17.6	0	0
6	Cu1Mn1-600	17.6	17.2	14.8	56.9	9.6	1.6
7	Cu1Mn1-700	17.4	14.6	16. 7	62.4	4.8	1.5
8	Cu1Mn1-700[c]	21.6	9.2	1.6	73.7	13.6	1.6
9	Cu1Mn1-800	6.5	30.5	26.5	42.5	0	0.5

[a]Reaction conditions: 1.0 g catalysts, 50 mL toluene, 1.0 MPa O_2 , 2 h, 190 °C.
[b]BAL = benzaldehyde; BOL = benzyl alcohol; BAC = benzoic acid; BB = benzyl benzoate.
[c]Reaction time = 3 h.

4. Conclusion

In the preparation of copper manganese oxides, different crystalline phases formed with different original Cu:Mn ratios, as determined by XRD. All the copper manganese oxides with different Cu:Mn ratios have the spinel phase $Cu_{1.5}Mn_{1.5}O_4$. CuO appeared in the copper-rich samples while the manganese-rich samples contained Mn_2O_3 phase. Copper manganese oxides with the Cu:Mn ratio of 1:1 would form spinel $Cu_{1.5}Mn_{1.5}O_4$ when calcined at temperatures above 500 °C. The $Cu_{1.5}Mn_{1.5}O_4$ crystallinity of the catalyst calcined at 600 °C is higher than that of the catalysts calcined at higher or lower temperatures, as evidenced by XRD. Calcination at 800 °C caused the decomposition of $Cu_{1.5}Mn_{1.5}O_4$ to Mn_2O_3 and high-dispersed CuO, as confirmed by the results of XRD and TPR. From the TRP profiles of Cu–Mn oxides calcined at different

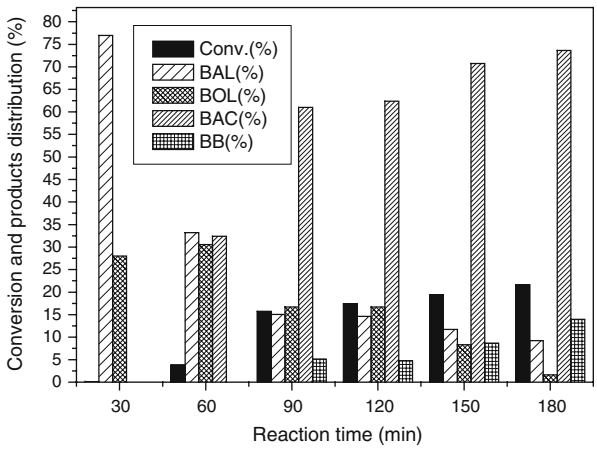

Figure 7. The product distributions at the different reaction time.

temperatures, we know that higher calcination temperature led to the less reducible samples.

The catalytic activities of copper manganese oxides were higher than other bimetallic oxides. Furthermore, the catalyst with the 1:1 of Cu:Mn ratio and calcined at 600 °C has the higher conversion of toluene and selectivity to benzoic acid. These results seem to suggest that the active phase is $Cu_{1.5}Mn_{1.5}O_4$.

The liquid-phase oxidation of toluene over heterogeneous catalyst was economic because the catalyst can be separated easily. At the same time the process is environmentally safer because of the advantage of heterogeneous system and the solvent-free condition.

Acknowledgments

We are grateful to the National Natural Science Foundation of China (Grant: 20233040) and the National High Technology Research and Development Program of China for the financial support (Grant: 2002AA321020, 2004GA321020).

References

[1] J. Thomas, R. Raja, G. Sankar and R.G. Bell, Nature 398 (1999) 227.
[2] J. Lozar, G. Falgayrac and A. Savall, Ind. Eng. Chem. Res. 40 (2001) 6055.
[3] A. Suresh, M. Sharma and T. Sridhar, Ind. Eng. Chem. Res. 39 (2000) 3958.
[4] T. Hirabayashi, S. Sakaguchi and Y. Ishii, Angew. Chem. Int. Ed. 43 (2004) 1120.
[5] H. Holtz and L. GardnerPhillips Petroleum Co., US Pat. 4088823 (1978) 1978.
[6] D. Bulushev, F. Rainone and L. Kiwi-Minsker, Catal. Today 96 (2004) 195.
[7] C. Freitag, S. Besselmann, E. Löffler, W. Grünert, F. Rosowski, M. Muhler, Catal. Today 91 (2004) 143.
[8] L. Kiwi-Minsker, D. Bulushev, F. Rainone and A.J. Renken, Molec. Catal. A: Chem. 184 (2002) 223.
[9] D. Bulushev, S. Reshetnikov, L. Kiwi-minsker and A. Renken, Appl. Catal. A: Gen. 220 (2001) 31.
[10] T. Bastock, J. Clark, K. Matin and B. Trenbirth, Green Chem. 4 (2002) 615.
[11] J. Zhu, A. Robertson, S. Tsang, Chem. Commun. (2002) 2044.
[12] J. Zhu and S.C. Tsang, Catal. Today 81 (2003) 673.
[13] M. Kantam, P. Sreekanth, K. Rao, T. Kumar, B. Rao and B Choudary, Catal. Lett. 81 (2002) 223.
[14] Y. Yoshino, Y. Hayashi, T. Iwahama, S. Sakaguchi and Y. Ishii, J. Org. Chem. 62 (1997) 6810.
[15] Y. Ishii, S. Sakaguchi and T. Iwahama, Adv. Synth. Catal. 343 (2001) 393.
[16] A. Lamb, W. Bray and J. Frazer, Ind. Eng. Chem. 12 (1920) 213.
[17] A. Mirzaei, R. Shaterian, M. Habibi, G. Hutchings and S. Taylor, Appl. Catal. A: Gen. 253 (2003) 499.
[18] H. Jones and H. Taylor, J. Phys. Chem. 27 (1923) 623.
[19] F.S. Stone, Adv. Catal. 5 (1962) 1.
[20] G. Hutchings, A. Mirzaei, R. Joyner, M. Siddiqui and S. Taylor, Catal. Lett. 42 (1996) 21.
[21] G. Hutchings, A. Mirzaei, R. Joyner, M. Siddiqui and S. Taylor, Appl. Catal. A: Gen. 166 (1998) 143.
[22] S. Kanungo, J. Catal. 58 (1979) 419.
[23] G. Schwab and S. Kanungo, J. Phys. Chem. NF. 107 (1977) 109.
[24] A. Wöllner, F. Lange, H. Schmelz and H. Knözinger, Appl. Catal. A: Gen. 94 (1993) 181.
[25] F. Wang, G. Yang, W. Zhang, W. Wu, J. Xu, Chem. Commun. (2003) 1172.
[26] F. Wang, G. Yang, W. Zhang, W. Wu and J. Xu, Adv. Synth. Catal 346 (2004) 633.
[27] G. Qi, X. Zheng, J. Fei and Z. Hou, J. Molec. Catal. A: Chem. 176 (2001) 195.
[28] I. Spassova, M. Khristova, D. Panayotov and D. Mehandjiev, J. Catal. 185 (1999) 43.
[29] B. Gillot, S. Buguet and Etienne Kester, J. Mater. Chem. 7 (1997) 2513.
[30] Y. Tanaka, T. Utaka, R. Kikuchi, T. Takeguchi, K. Sasaki and K. Eguchi, J. Catal. 215 (2003) 271.
[31] F. Buciuman, F. Patcas and T. Hahn, Chem. Eng. Proc. 38 (1999) 563.
[32] Y. Tanaka, T. Utaka, R. Kikuchi, K. Sasaki and K. Eguchi, Appl. Catal. A: Gen. 242 (2003) 285.
[33] I. Spasspval and D. Mehandjiev, React. Kinet. Catal. Lett. 58 (1996) 57.
[34] I. Leith and M. Howden, Appl. Catal. A: Gen. 37 (1992) 75.